Published in final edited form as:
Cell Metab. 2014 April 1; 19(4): 694–701. doi:10.1016/j.cmet.2014.03.009.

Adenovirus E4ORF1-induced MYC activation promotes host cell anabolic glucose metabolism and virus replication

Minh Thai[1], **Nicholas A Graham**[1,2], **Daniel Braas**[1,3], **Michael Nehil**[4], **Evangelia Komisopoulou**[1,2], **Siavash K. Kurdistani**[5,6,7], **Frank McCormick**[4], **Thomas G. Graeber**[1,2,3,6], and **Heather R. Christofk**[1,3,6,7]

[1]Department of Molecular and Medical Pharmacology, David Geffen School of Medicine, University of California, Los Angeles, Los Angeles, CA 90095, USA

[2]Crump Institute for Molecular Imaging, David Geffen School of Medicine, University of California, Los Angeles, Los Angeles, CA 90095, USA

[3]UCLA Metabolomics Center, University of California, Los Angeles, Los Angeles, CA 90095, USA

[4]Helen Diller Family Comprehensive Cancer Center, University of California, San Francisco School of Medicine, San Francisco, CA 94158, USA

[5]Department of Biological Chemistry, David Geffen School of Medicine, University of California, Los Angeles, Los Angeles, CA 90095, USA

[6]Jonsson Comprehensive Cancer Center, David Geffen School of Medicine, University of California, Los Angeles, Los Angeles, CA 90095, USA

[7]Eli and Edythe Broad Center of Regenerative Medicine and Stem Cell Research, University of California, Los Angeles, Los Angeles, CA 90095, USA

SUMMARY

Virus infections trigger metabolic changes in host cells that support the bioenergetic and biosynthetic demands of viral replication. While recent studies have characterized virus-induced changes in host cell metabolism (Munger et al., 2008; Terry et al., 2012), the molecular mechanisms by which viruses reprogram cellular metabolism have remained elusive. Here we show that the gene product of adenovirus E4ORF1 is necessary for adenovirus-induced upregulation of host cell glucose metabolism and sufficient to promote enhanced glycolysis in cultured epithelial cells by activation of MYC. E4ORF1 localizes to the nucleus, binds to MYC, and enhances MYC binding to glycolytic target genes, resulting in elevated expression of specific glycolytic enzymes. E4ORF1 activation of MYC promotes increased nucleotide biosynthesis from glucose intermediates and enables optimal adenovirus replication in primary lung epithelial cells.

*Corresponding author: hchristofk@mednet.ucla.edu; Phone: (310) 794-4248.

Our findings show how a viral protein exploits host cell machinery to reprogram cellular metabolism and promote optimal progeny virion generation.

INTRODUCTION

Similar to infection with certain other viruses (Diamond et al., 2010; Munger et al., 2008; Vastag et al., 2011), adenovirus infection increases host cell glycolytic metabolism even in the presence of ample oxygen for oxidative metabolism, thus mirroring the Warburg effect in cancer (Fisher and Ginsberg, 1957; Warburg, 1956). Adenoviral proteins and tumor cell mutations are known to converge in perturbing many of the same molecular players to execute their programs of growth deregulation and limitless propagation (O'Shea, 2005). Consequently, adenoviruses can be used as a genetically tractable tool to gain new insights into the complex networks that underlie both this metabolic switch and aberrant cellular replication. Since both adenoviruses and oncogenes rewire cellular metabolism to satisfy the demands of increased proliferation of virions and daughter cells, respectively, studying the mechanism by which adenovirus reprograms host cell glucose metabolism may reveal key nodes important for upregulation of anabolic glucose metabolism in cancer.

RESULTS

Adenovirus infection increases glycolytic metabolism of host cells

To confirm that adenovirus infection enhances glycolytic metabolism of cultured epithelial cells, we infected the non-tumorigenic breast epithelial cell line MCF10A with a wild-type strain of Adenovirus 5 (AD WT). AD WT infection robustly increases glycolytic metabolism of MCF10A cells, visibly evident by acidification of the culture media and yellowing of the pH indicator phenol red (Figure 1A), and quantifiably evident by elevated glucose consumption and lactate production rates over multiple days post infection (Figures 1B, C). MCF10A cells infected with AD WT also exhibited a dramatic reduction in oxygen consumption rate (Figure 1D), suggesting decreased reliance on oxidative phosphorylation. These observed changes in MCF10A metabolism upon AD WT infection were not due to differences in cell number or apoptosis (Figure S1).

To identify adenoviral gene elements necessary for upregulation of glycolytic metabolism in host cells, we tested Adenovirus 5 deletion mutants for their competence to alter glucose consumption, lactate production, and oxygen consumption rates. A replication-deficient adenovirus deletion mutant lacking the entire E4 early transcription unit region (AD ΔE4) failed to increase glycolytic metabolism and decrease respiration in infected cells (Figures 1A–D). Notably, stable expression of the entire Ad5 E4 region in MCF10A cells was sufficient to increase glucose consumption and lactate production rates, but had no effect on oxygen consumption rates (Figure 1E). Together, these data suggest that the E4 region is necessary for adenovirus-induced enhancement of host cell glucose metabolism, and is sufficient to promote increased glycolysis, but not decreased respiration, in MCF10A cells.

Adenoviral gene product E4ORF1 is sufficient to promote increased glucose metabolism in epithelial cells

The E4 region encodes at least six distinct polypeptides, defined as E4ORF 1–6 (Figure S2A), which regulate viral DNA synthesis and viral gene expression (Javier, 1994). To determine which E4ORF is responsible for the observed increase in glycolytic flux in response to gene expression from the E4 region, each of five of the E4ORFs was individually expressed in MCF10A cells (Figure 2A). The splice variant, E4ORF6/7 was not expressed, and its role in these metabolic changes cannot be excluded. By measuring glucose consumption and lactate production rates, we found that only E4ORF1 expression, by itself, was sufficient to increase cellular glycolytic flux (Figure 2B).

Among the E4ORFs individually expressed in Figure 2A, E4ORF1 and E4ORF6 were expressed at lower levels than the other ORFs. Because ORF6 plays a role in facilitating viral gene expression from the onset of late phase (Dix and Leppard, 1993), we reasoned that co-expressing ORF6 may enhance expression or stability of ORF1. Indeed, when both ORF1 and ORF6 were expressed together in MCF10A cells, ORF1 protein levels were robustly elevated, and we found that ORF1 and ORF6 physically interacted (Figure S2B). Since these data suggest that E4ORF6 binds to and stabilizes E4ORF1, we stably co-expressed E4ORF6 along with E4ORF1 in all subsequent experiments.

Adenovirus 5 E4ORF1 encodes a 14-kDa polypeptide previously shown to induce transformation and enhance tumorigenicity of rat embryonic fibroblasts (Javier, 1994). The tumorigenic potential of E4ORF1 depends on a C-terminal PDZ domain binding motif that mediates binding to a select group of cellular PDZ domain-containing proteins (Chung et al., 2007) and activation of PI3K and AKT (Frese et al., 2003). We initially hypothesized that E4ORF1 increases glycolytic flux through activation of PI3K signaling. However, a tetracycline-inducible truncation mutant of E4ORF1 lacking the PDZ binding motif was as capable as full length E4ORF1 at increasing glucose consumption and lactate production rates in MCF10A cells when acutely expressed following addition of doxycycline (Figures 2C, D). These results suggest that E4ORF1 enhances cellular glycolytic metabolism in a PI3K-independent manner.

MYC transcriptional activity is enhanced by E4ORF1 expression and adenovirus infection

To gain insight into the mechanism by which E4ORF1 promotes increased glycolytic flux, we conducted a global microarray analysis of changes in whole genome expression in E4ORF6-expressing MCF10A cells that were induced to express E4ORF1 versus an empty vector control. Using Gene Set Enrichment Analysis (GSEA), we found MYC-regulated genes were significantly enriched in cells expressing E4ORF1 (Table S1, Figure S3A, $p<0.001$). In addition, gene sets with increased MYC activity were also enriched when compared to all gene sets (Figure S3B, $p<0.001$). It was recently reported that tumor viruses rewire host cell transcriptome networks (Rozenblatt-Rosen et al., 2012). Comparing our E4ORF1 gene expression signature to that of E4ORF1 in IMR90 human diploid fibroblasts, we found that MYC gene sets are coordinately regulated by E4ORF1 in both contexts (Figure S3C, $p<0.001$). Analysis of MYC gene sets relative to all gene sets confirmed

enrichment of MYC gene sets in both breast epithelial and primary fibroblast systems (Figure S3D).

To investigate whether MYC is indeed affected by E4ORF1 expression in MCF10A cells, as suggested from our enrichment analysis, we first examined localization of MYC in E4ORF1- versus empty vector-expressing cells. As shown in Figure 3A, we found that nuclear MYC protein levels are elevated in E4ORF1-expressing cells. Additionally, E4ORF1 physically associates with MYC and E4ORF6 in the nuclear fraction (Figure 3B). Since E4ORF6 is unable to interact with MYC in the absence of E4ORF1 expression, binding between MYC and the E4ORF proteins depends on interaction with E4ORF1 (Figure 3B). Since MYC is a transcription factor that regulates energy metabolism through direct activation of metabolic genes (Osthus et al., 2000; Shim et al., 1997), we reasoned that E4ORF1 expression and binding to MYC may enhance MYC activation of glycolytic genes. To test this hypothesis we measured, by chromatin immunoprecipitation and quantitative PCR (ChIP-qPCR), MYC binding to candidate glycolytic target genes. As shown in Figure 3C, MYC binding to glycolytic target genes is elevated in cells induced to express E4ORF1 versus the empty vector control (Fisher's method $p<0.001$). Additionally, E4ORF1 itself also binds to MYC glycolytic target genes (Fisher's method $p<0.001$) (Figures 3C and S3E).

Previous findings suggest that the oncogenic potential of E4ORF1 depends not only on the PDZ binding motif, but also on a second protein element called region 2 (Chung et al., 2007). We generated and tested a series of E4ORF1 region 2 point mutants for their capability to enhance glycolytic metabolism (data not shown). One region 2 mutant, E4ORF1 D68A, exhibits a severe defect in cellular transformation, retains the capacity to bind to cellular PDZ proteins, but fails to stimulate the PI3K pathway (Chung et al., 2007). We generated MCF10A cells that inducibly express E4ORF1 D68A or wild-type E4ORF1 (E4ORF1 WT) at similar protein expression levels (Figure 3A). The D68A point mutation in E4ORF1 abolished the increased glycolytic flux observed with E4ORF1 WT expression (Figure 3D). Additionally, D68A mutation impaired the ability of E4ORF1 to elevate nuclear MYC levels (Figure 3A), interact with nuclear MYC (Figure 3B), bind to MYC glycolytic target genes (Fisher's method $p = 0.06$) (Figures 3C and S3E), and promote increased MYC binding to glycolytic target genes (Fisher's method $p = 0.09$) (Figures 3C and S3E).

To investigate whether the observed increase in MYC binding to glycolytic target genes in E4ORF1-expressing cells results in increased expression of glycolytic genes, we measured relative mRNA levels of glycolytic target genes in cells expressing E4ORF1 WT and E4ORF1 D68A versus empty vector. Expression of the first two rate-limiting and glycolysis promoting (as opposed to gluconeogenesis) enzymes in the glycolytic pathway, Hexokinase 2 (HK2) and Phosphofructokinase 1 (PFKM), was significantly elevated in E4ORF1-expressing cells (Figure 3E). Additionally, E4ORF1 D68A-expressing cells expressed lower levels of HK2 and PFKM mRNAs than E4ORF1 WT-expressing cells (Figure 3E). Paradoxically, although MYC binding to the GAPDH and LDHA gene loci was significantly elevated in E4ORF1-expressing cells (Figures 3C and S3E), no increase in GAPDH and LDHA mRNA levels was observed. However, since the D68A mutation impaired E4ORF1's

capability to both activate MYC-induced transcription of HK2 and PFKM and promote increased glycolysis in MCF10A cells, these data lend further support to the model that E4ORF1 promotes enhanced glycolysis through binding to MYC and activation of MYC-induced transcription of glycolytic genes.

To determine whether E4ORF1 promotes MYC-induced transcription of glycolytic genes during adenovirus infection, we generated a mutant of Adenovirus 5 that contains the D68A amino acid alteration in E4ORF1 (AD ORF1 D68A) and compared its effects to wild type virus (AD WT) on mediating MYC transcription of metabolic genes. AD WT infection of primary Normal Human Bronchial Epithelial (NHBE) cells leads to enrichment of MYC binding to its glycolytic target genes, HK2 and PFKM (Figures 3F and S3F). This elevated binding is abrogated when the cells are instead infected with AD ORF1 D68A (Figures 3F and S3F). Additionally, cells infected with AD WT, but not AD ORF1 D68A, exhibit increased expression of HK2 and PFKM1 mRNA (Figure 3G). Together, these data suggest that E4ORF1 modulates MYC transcription of glycolytic genes during adenovirus infection.

E4ORF1 activation of MYC promotes anabolic glucose metabolism and optimal adenovirus replication

To examine whether the increase in host cell glycolysis accomplished by E4ORF1 activation of MYC is important for adenovirus replication, we first prevented MYC activation in adenovirus-infected primary Normal Human Bronchial Epithelial (NHBE) cells by short hairpin RNA (shRNA)-mediated knockdown of MYC expression. MYC knockdown diminished the acidification of the growth medium (Figure 4A) and blocked the elevation in glucose consumption and lactate production rates conferred by adenovirus infection (Figure 4B). Moreover, the plaque forming capacity of virus harvested from NHBE cells expressing MYC shRNA was reduced by an order of magnitude when compared to virus harvested from cells expressing a scrambled shRNA control (Figure 4C). These data suggest that MYC-activated metabolic changes contribute to optimal adenovirus replication in primary cells.

To specifically address whether E4ORF1-induced activation of MYC is necessary for optimal adenovirus replication, we infected NHBE cells with AD ORF1 D68A and compared the effects of this mutant virus to those of AD WT on cell metabolism and virus replication. Similar to AD ΔE4 (Figures 1A–C), AD ORF1 D68A was unable to enhance glycolytic flux of infected cells (Figures 4D, E). Progeny virus harvested from AD ORF1 D68A-infected NHBE cells formed significantly fewer plaques in HeLa cells than progeny virus harvested from AD WT-infected cells (Figure 4F). To determine whether the observed replication deficiency of the AD ORF1 D68A mutant virus was due to its inability to activate PI3K or enhance glycolytic flux, we also compared the effects of AD WT versus AD ORF1 D68A infection on virus replication in MCF10A cells, a relatively more glycolytic cell line than NHBE cells with low basal PI3K activation (Figure 2C and Figures S4A, B). Progeny virus harvested from AD ORF1 D68A-infected MCF10A cells formed a similar number of plaques in HeLa cells than progeny virus harvested from AD WT-infected cells (Figure S4C), suggesting that the increased glycolysis in MCF10A cells rescued the replication deficiency of the AD ORF1 D68A virus. Together these data imply that

E4ORF1-induced activation of MYC and enhancement of glycolytic flux promotes optimal adenovirus replication in host cells.

Since adenovirus is a non-enveloped DNA virus, we hypothesized that E4ORF1/MYC-enhanced glycolytic metabolism may contribute to adenovirus replication by enabling increased nucleotide biosynthesis from glucose metabolites. To test this hypothesis, we labeled NHBE cells with [1,2-^{13}C]-glucose, and measured the fraction of ^{13}C-labeled nucleotides in AD WT- versus AD ORF1D68A-infected NHBE cells. NHBE cells infected with AD WT, but not AD ORF1D68A, exhibited a robust increase in the incorporation of ^{13}C from glucose into nucleotides (Figure 4G). AD WT-infected cells also showed increased levels of nucleotides and nucleotide metabolism intermediates relative to AD ORF1D68A-infected cells and mock-infected cells (Figure S4D). To probe whether the increased nucleotide biosynthesis from glucose metabolites in adenovirus-infected cells contributes to DNA replication, we labeled NHBE cells with [U-^{14}C]-glucose, and measured the fraction of ^{14}C-labeled DNA in mock-infected, AD WT-infected, and AD ORF1D68A-infected cells. As shown in Figure S4E, AD WT infection, but not AD ORF1D68A infection, resulted in increased incorporation of labeled glucose carbons into DNA. These results suggest that E4ORF1-induced activation of MYC during adenovirus infection leads to increased nucleotide biosynthesis from glucose for elevated DNA replication, implying potentially increased flux of glucose metabolites through the pentose phosphate pathway to generate ribose-5-phosphate. Consistent with this hypothesis, we found that mRNA expression levels of RPIA and RPE, enzymes that regulate carbon exchange reactions in the non-oxidative arm of the pentose phosphate pathway, are significantly increased in cells expressing E4 ORF1 WT, but not E4 ORF1 D68A (Figures S4F). Moreover, in the context of virus infection, we also observed that RPIA and RPE mRNA levels are elevated in NHBE cells infected with AD WT, but not AD ORF1D68A (Figure 4H). Together these data support a model whereby E4ORF1-induced activation of MYC during adenovirus infection leads to increased flux through glycolysis and potentially through the non-oxidative arm of the pentose phosphate pathway to provide nucleotides for adenoviral DNA replication (Figure 4I).

DISCUSSION

This study presents a molecular mechanism by which a virus reprograms host cell metabolism to promote replication: adenovirus E4ORF1-induced activation of MYC. However, the precise mechanism by which E4ORF1 enhances MYC-dependent transcription of metabolic genes remains to be determined. Our results suggest that E4ORF1 binds to MYC and leads to increased MYC localization to glycolytic target genes. E4ORF1 may promote MYC activation by increasing affinity of MYC for specific metabolic target genes, promoting binding of chromatin remodeling machinery to enhance MYC-induced transcription, or simply by enhancing MYC protein stability. It will be interesting for future studies to determine both how E4ORF1 induces MYC-dependent transcription of metabolic genes during adenovirus infection and whether MYC plays a role in metabolic reprogramming by other types of viruses.

Although MYC is known to regulate transcription of many glycolytic genes, our data suggests that E4ORF1-induced activation of MYC most notably enhances transcription of HK2 and PFKM during adenovirus infection. Since viruses undergo selective pressure for efficiency, only key flux-altering enzymes are likely elevated during infection. Our data suggests that elevated HK2 and PFKM levels are sufficient to drive the increased glycolysis observed upon E4ORF1 expression. Consistent with this hypothesis, hexokinase activity is elevated in E4ORF1 but not E4ORF1 D68A-expressing MCF10A cells (Figure S4G), and during AD WT but not AD ORF1D68A infection of NHBE cells (Figure S4H). Additionally, stable expression of HK2, by itself, in MCF10A cells is sufficient to enhance glycolysis to a similar extent as stable expression of E4ORF1 or MYC (Figures S4I–K). This data suggests that elevated HK2 activity may underlie the increased glycolytic flux induced by E4ORF1 activation of MYC, and that viruses may be useful tools to reveal key enzymes important for pathway fluxes. However, further studies are needed to determine whether HK2 elevation during adenovirus infection is necessary for increased host cell glycolysis and virus replication.

While our data suggest that E4ORF1-induced MYC activation is necessary for increased glycolytic metabolism in AD-infected cells, another virus-encoded protein (or combination of viral proteins) is responsible for abrogation of host cell respiration upon adenovirus infection (shown in Figure 1D) which likely contributes to the greater increase in glycolysis observed during adenovirus infection versus stable E4ORF1 expression (Figures 1B, C versus Figure 2B). Preliminary data suggest that host cell mitochondria are intact and membrane potential is maintained following AD-infection, despite the substantially reduced oxygen consumption rate (data not shown). It will be interesting to determine the viral components responsible for this decrease in cellular respiration and whether these viral components, and this metabolic alteration, also contribute to adenovirus replication.

Our results support MYC as a key node in promoting cellular anabolic glucose metabolism. Consistent with our data in adenovirus-infected cells, recent studies have shown that MYC activation downstream of oncogenic Kras reprograms tumor metabolism towards increased glycolysis and shunting of glucose metabolites towards the non-oxidative arm of the PPP for ribose generation (Ying et al., 2012), and that MYC upregulation contributes to the Warburg effect in breast cancer patient tumors (Palaskas et al., 2011). MYC-dependent transcription has also been implicated in metabolic reprogramming towards increased glycolysis and glutaminolysis to support biosynthesis during activation of primary T lymphocytes (Wang et al., 2011). Collectively, our results and these studies indicate that MYC-dependent transcription of metabolic genes is a general mechanism, active across multiple patho-physiological conditions, by which cells reprogram metabolism towards increased anabolism.

EXPERIMENTAL PROCEDURES

Measurement of glucose consumption rates and lactate production rates

Cellular glucose consumption and lactate export rates were measured using a Nova Biomedical Bioprofile Basic Analyzer. Briefly, cells were seeded in triplicate in 6-well plates at 50% confluency to ensure the measurements would be taken when the cells were

subconfluent. Twenty-four hours post seeding, the media was refreshed for all cells, and media was added to empty wells as a blank control. After 24hr incubation, 1ml of media was removed from each sample and the blank control, and media samples were analyzed in the Nova Bioprofile analyzer. Cell number was determined using a Coulter particle analyzer, and used to normalize the calculated rates.

Enrichment Analysis

To identify gene sets enriched in E4ORF1-expressing MCF10A cells, we used the gene set enrichment analysis (GSEA) algorithm (Subramanian et al., 2005) with pathway annotation defined by the Molecular Signatures Database (MSigDB) C2 collection (version 2.5) of canonical signaling pathways, cellular processes, chemical and genetic perturbations, and human disease states. Probesets were ranked by the signal-to-noise ratio (SNR) between E4ORF1- and vector-expressing cells (n = 3 for each condition) and collapsed by the maximum absolute SNR for each gene. To identify the enrichment of MYC targets in E4ORF1-expressing cells, we manually curated the MSigDB genes sets associated with increased or decreased MYC activity (“Myc up” and “Myc down”, n = 26 and 13, respectively). We then ranked all gene sets by average NES-ranked and calculated the probability that “Myc up” and “Myc down” pathways were enriched using a GSEA-style enrichment analysis. We have deposited the gene expression data in GEO. The accession number is GSE52998.

Plaque Assay

4×10^6 NHBE cells were infected at 10 PFU/cell for 5 days. Cells from the entire plate were harvested by pipetting up and down, collected in a conical tube, and spun down at 3K for 10 minutes. Pellet was resuspended with 100μL 10mM Tris pH 7.4. Cells were lysed by freeze, thaw and vortexing vigorously. Supernatant was harvested as virus stocks for plaque assays. For viral replication assays, HeLa cells were grown to 80% confluence and subsequently infected with 10-fold dilutions of virus stocks. Dilutions of virus stocks were added to cells in duplicate. Plates were then overlayed with Dulbecco’s modified Eagle’s medium (DMEM) containing 0.7% agarose. Plaques were counted when visible to the naked eye, typically 5 days. Titer was calculated in plaque forming units (PFU) per mL.

Statistical Analysis

All data are presented as mean +/− SEM. As noted in figure legends, data were analyzed by two-sample equal variance Student’s t-test with two-tailed analysis.

Supplementary Material

Refer to Web version on PubMed Central for supplementary material.

Acknowledgments

We thank C. Eng and A. Berk for helpful advice with adenovirus preparations and assays. We thank C. Jacobs for technical assistance. We thank J. Byrne for designing the model figure. We thank H. Herschman for comments on the manuscript. M.T. is a postdoctoral trainee supported by the National Cancer Institute of the National Institutes of Health under Award Number T32-CA009120-37. N.A.G. is a postdoctoral trainee supported by the UCLA Scholars in Oncologic Molecular Imagining (SOMI) program, the UCLA Tumor Cell Biology Program, the NIH

grant R25T CA098010, and the United States Health and Human Services Ruth L. Kirschstein Institutional National Research Service Award T32 CA 009056. T.G.G. is supported by the NCI/NIH (P01 CA168585, R21 CA169993), an American Cancer Society Research Scholar Award (RSG-12-257-01-TBE), the CalTech-UCLA Joint Center for Translational Medicine, the National Center for Advancing Translational Sciences UCLA CTSI Grant UL1TR000124, and a Concern Fondation CONquer CanCER Now Award. H.R.C. is supported by the Searle Scholars Program, the NIH Director's New Innovator Award (DP2OD008454-01), the Caltech/UCLA Nanosystems Biology Cancer Center (NCI U54 CA151819), and a UCLA Broad Stem Cell Research Center – Concern Foundation Research Award.

References

Chung S-H, Frese KK, Weiss RS, Prasad BVV, Javier RT. A New Crucial Protein Interaction Element That Targets the Adenovirus E4-ORF1 Oncoprotein to Membrane Vesicles. J Virol. 2007; 81:4787–4797. [PubMed: 17314165]

Diamond DL, Syder AJ, Jacobs JM, Sorensen CM, Walters KA, Proll SC, McDermott JE, Gritsenko MA, Zhang Q, Zhao R, et al. Temporal Proteome and Lipidome Profiles Reveal Hepatitis C Virus-Associated Reprogramming of Hepatocellular Metabolism and Bioenergetics. PLoS Pathog. 2010; 6:e1000719. [PubMed: 20062526]

Dix I, Leppard KN. Regulated splicing of adenovirus type 5 E4 transcripts and regulated cytoplasmic accumulation of E4 mRNA. J Virol. 1993; 67:3226–3231. [PubMed: 8497048]

Fisher TN, Ginsberg HS. Accumulation of organic acids by HeLa cells infected with type 4 adenovirus. Proc Soc Exp Biol Med. 1957; 95:47–51. [PubMed: 13431982]

Frese KK, Lee SS, Thomas DL, Latorre IJ, Weiss RS, Glaunsinger BA, Javier RT. Selective PDZ protein-dependent stimulation of phosphatidylinositol 3-kinase by the adenovirus E4-ORF1 oncoprotein. Oncogene. 2003; 22:710–721. [PubMed: 12569363]

Javier RT. Adenovirus type 9 E4 open reading frame 1 encodes a transforming protein required for the production of mammary tumors in rats. J Virol. 1994; 68:3917–3924. [PubMed: 8189528]

Munger J, Bennett BD, Parikh A, Feng XJ, McArdle J, Rabitz HA, Shenk T, Rabinowitz JD. Systems-level metabolic flux profiling identifies fatty acid synthesis as a target for antiviral therapy. Nat Biotechnol. 2008; 26:1179–1186. [PubMed: 18820684]

O'Shea CC. Viruses – seeking and destroying the tumor program. Oncogene. 2005; 24:7640–7655. [PubMed: 16299526]

Osthus RC, Shim H, Kim S, Li Q, Reddy R, Mukherjee M, Xu Y, Wonsey D, Lee LA, Dang CV. Deregulation of glucose transporter 1 and glycolytic gene expression by c-Myc. J Biol Chem. 2000; 275:21797–21800. [PubMed: 10823814]

Palaskas N, Larson SM, Schultz N, Komisopoulou E, Wong J, Rohle D, Campos C, Yannuzzi N, Osborne JR, Linkov I, et al. 18F-fluorodeoxy-glucose positron emission tomography marks MYC-overexpressing human basal-like breast cancers. Cancer Res. 2011; 71:5164–5174. [PubMed: 21646475]

Rozenblatt-Rosen O, Deo RC, Padi M, Adelmant G, Calderwood MA, Rolland T, Grace M, Dricot A, Askenazi M, Tavares M, et al. Interpreting cancer genomes using systematic host network perturbations by tumour virus proteins. Nature. 2012; 487:491–495. [PubMed: 22810586]

Shim H, Dolde C, Lewis BC, Wu CS, Dang G, Jungmann RA, Dalla-Favera R, Dang CV. c-Myc transactivation of LDH-A: implications for tumor metabolism and growth. Proc Natl Acad Sci USA. 1997; 94:6658–6663. [PubMed: 9192621]

Subramanian A, Tamayo P, Mootha VK, Mukherjee S, Ebert BL, Gillette MA, Paulovich A, Pomeroy SL, Golub TR, Lander ES, et al. Gene set enrichment analysis: a knowledge-based approach for interpreting genome-wide expression profiles. Proc Natl Acad Sci USA. 2005; 102:15545–15550. [PubMed: 16199517]

Terry LJ, Vastag L, Rabinowitz JD, Shenk T. Human kinome profiling identifies a requirement for AMP-activated protein kinase during human cytomegalovirus infection. Proc Natl Acad Sci USA. 2012; 109:3071–3076. [PubMed: 22315427]

Vastag L, Koyuncu E, Grady SL, Shenk TE, Rabinowitz JD. Divergent Effects of Human Cytomegalovirus and Herpes Simplex Virus-1 on Cellular Metabolism. PLoS Pathog. 2011; 7:e1002124. [PubMed: 21779165]

Wang R, Dillon CP, Shi LZ, Milasta S, Carter R, Finkelstein D, McCormick LL, Fitzgerald P, Chi H, Munger J, et al. The Transcription Factor Myc Controls Metabolic Reprogramming upon T Lymphocyte Activation. Immunity. 2011; 35:871–882. [PubMed: 22195744]

Warburg O. On respiratory impairment in cancer cells. Science. 1956; 124:269–270. [PubMed: 13351639]

Ying H, Kimmelman AC, Lyssiotis CA, Hua S, Chu GC, Fletcher-Sananikone E, Locasale JW, Son J, Zhang H, Coloff JL, et al. Oncogenic Kras Maintains Pancreatic Tumors through Regulation of Anabolic Glucose Metabolism. Cell. 2012; 149:656–670. [PubMed: 22541435]

Yuan J, Bennett BD, Rabinowitz JD. Kinetic flux profiling for quantitation of cellular metabolic fluxes. Nat Protoc. 2008; 3:1328–1340. [PubMed: 18714301]

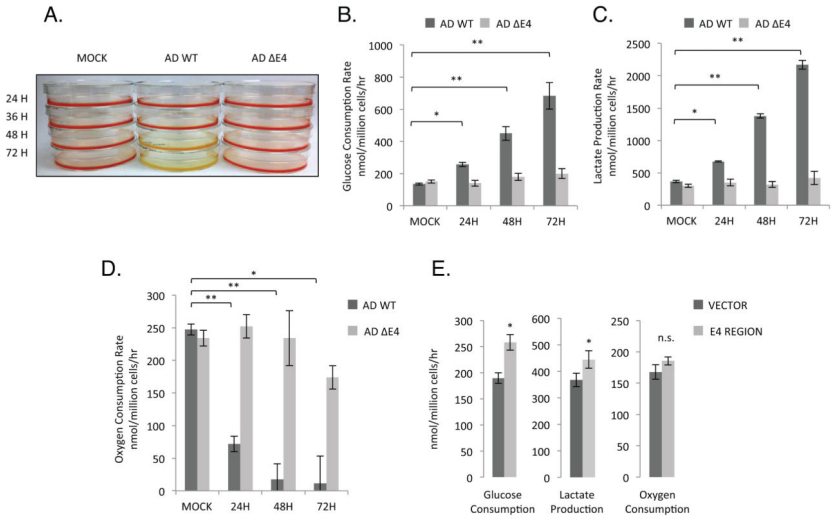

Figure 1. The E4 region is necessary for adenovirus-induced enhancement of glucose metabolism in host cells

(A) MCF10A cells were either mock infected, or infected with AD WT or AD ΔE4 virus for the indicated times. Yellowing of the pH indicator dye phenol red depicts media acidification from enhanced lactic acid production by the AD WT-infected cells. The average cell numbers at 72 hours for mock, WT, and ΔE4 infections are 5.8×10^6, 3.2×10^6, and 3.8×10^6, respectively. In **(B)–(D)** MCF10A cells were infected for the indicated times, and metabolic measurements were taken. Glucose consumption rates (**B**), lactate production rates (**C**), and oxygen consumption rates (**D**) from cells infected with AD WT or AD ΔE4 were measured in triplicate samples. **(E)** Metabolic measurements from MCF10A cells constitutively expressing a vector control or the full E4 region. Error bars denote standard errors of the mean (n=3). * denotes $p<0.05$; ** denotes $p<0.01$.

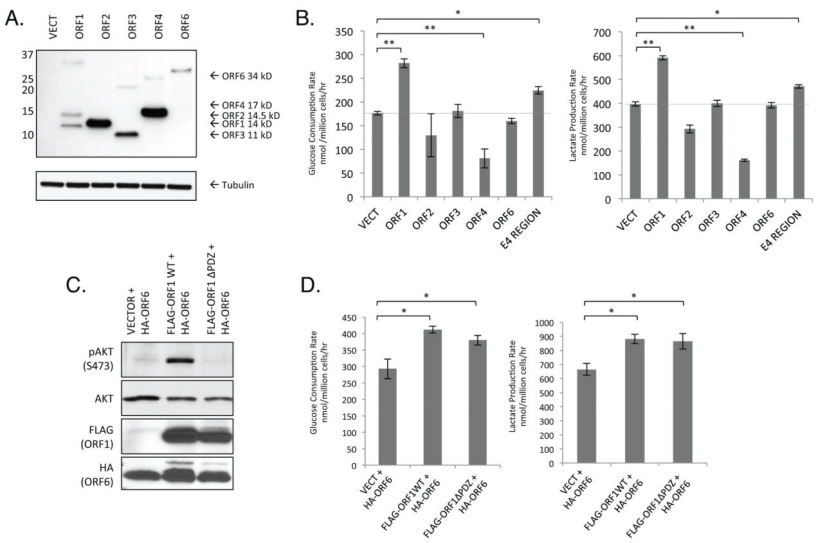

Figure 2. The adenoviral gene product E4ORF1 is sufficient to promote increased glucose metabolism in cultured epithelial cells

(A) Immunoblotting of lysates from MCF10A cells stably expressing flag-tagged E4 ORF1, ORF2, ORF3, ORF4, or ORF6. The top panel was probed with FLAG antibody, and the bottom panel was probed with tubulin antibody to control for loading. **(B)** Glucose consumption and lactate production rates from MCF10A cells stably expressing the flag-tagged ORFs indicated in (A). **(C)** Immunoblotting of lysates from MCF10A cells stably expressing HA-tagged E4ORF6 along with an inducible empty vector, flag-tagged ORF1 WT, or flag-tagged ORF1ΔPDZ. Briefly, the cells were treated with 1ug ml^{-1} doxycycline for 24 hours and subsequently starved for 24 hours in serum-free media with 1ug ml^{-1} doxycycline. To test the activation of PI3K, lysates were probed for phospho-Ser473-AKT; total AKT was used as a loading control, and FLAG was used to indicate induced ORF1 expression. **(D)** Cells described in (C) were induced to express flag-tagged ORF1 WT or flag-tagged ORF1ΔPDZ, and glucose consumption and lactate production rates were measured in full serum conditions. Error bars denote standard errors of the mean (n=3). * denotes $p<0.05$; ** denotes $p<0.01$.

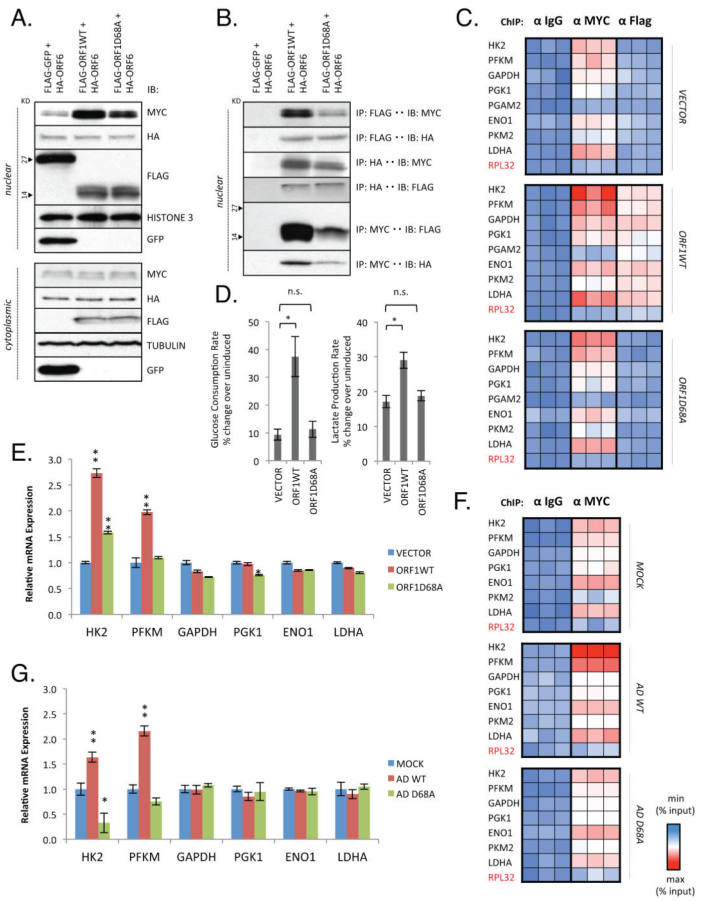

Figure 3. E4ORF1 enhances MYC transcriptional activation of glycolytic genes

(A) Immunoblotting (IB) of nuclear and cytoplasmic fractions from HA-tagged E4ORF6-expressing MCF10A cells induced to express vector control, flag-tagged E4ORF1 (ORF1WT), or the flag-tagged E4ORF1 D68A point mutant (ORF1D68A). Lysates were clonally selected to have equal molar amounts of E4ORF1 proteins. **(B)** Immunoprecipitations (IP) from nuclear fractions of HA-tagged E4ORF6-expressing MCF10A cells expressing FLAG-GFP or induced to express flag-tagged ORF1WT or flag-tagged ORF1D68A. **(C)** Heatmap depicts the level of MYC binding to the indicated genes by ChIP-qPCR in HA-tagged E4ORF6-expressing MCF10A cells induced to express vector control, flag-tagged ORF1WT, or flag-tagged ORF1D68A using antibodies towards MYC, FLAG, or IgG as a negative control. RLP32 is used as a negative control locus for MYC. The ChIP values represent the amount of immunoprecipitated DNA in each sample relative to the total amount of input chromatin (equivalent to 1) and color-coded with a gradient from blue for the minimum through red for the maximum percent of input. Each square is an independent experiment with 3 replicates. Specific values for % input can be found in Figure S3E. **(D)** Relative glucose consumption and lactate production rates from HA-tagged E4ORF6-expressing MCF10A cells induced to express equal levels of ORF1WT or ORF1D68A compared to respective uninduced samples. **(E)** Relative mRNA levels of glycolytic genes from HA-tagged E4ORF6-expressing MCF10A cells induced to express empty vector, E4ORF1 WT or E4ORF1 D68A. **(F)** Heatmap representing MYC binding to

indicated gene targets by ChIP-qPCR in NHBE cells infected with AD WT or AD E4ORF1D68A for 4 hours at equal titers. Specific values for % input can be found in Figure S3F. **(G)** Relative mRNA levels of glycolytic genes from NHBE cells infected with AD WT or AD D68A for 4 hours at equal titers. For (D), (E) and (G), error bars denote standard errors of the mean (n=3). * denotes $p<0.05$; ** denotes $p<0.01$.

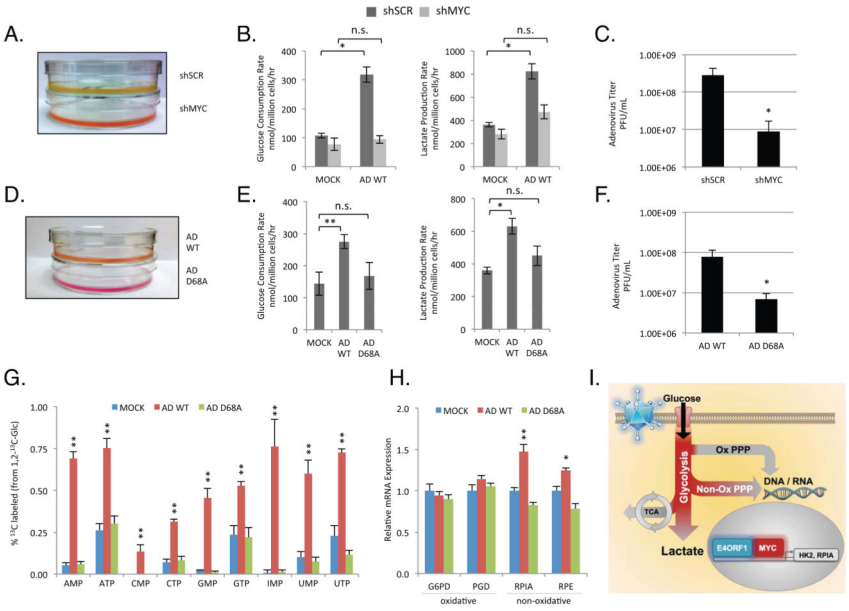

Figure 4. E4ORF1 activation of MYC promotes anabolic glucose metabolism and optimal adenovirus replication

(A) AD WT-infected NHBE cells stably expressing a MYC-directed shRNA exhibit less yellowing of the media pH indicator dye phenol red than AD WT-infected NHBE cells stably expressing a scrambled shRNA control. **(B)** Glucose consumption and lactate production rates from NHBE cells expressing scrambled shRNA (dark grey) or MYC shRNA (light grey) 24 hours post infection with AD WT versus mock infection. **(C)** Progeny virus was harvested from AD WT-infected NHBE cells expressing scrambled shRNA or MYC shRNA, and adenovirus titers were determined using serial plaque assays on HeLa monolayers. **(D)** AD D68A-infected NHBE cells exhibit less yellowing of the media pH indicator dye phenol red than AD WT-infected cells. **(E)** Glucose consumption and lactate production rates from NHBE cells mock infected or infected with AD WT or AD D68A. **(F)** Progeny virus from AD WT- and AD D68A-infected NHBE cells was harvested and adenovirus titers were determined as in (C). **(G)** NHBE cells mock infected or infected with AD WT or AD D68A were cultured in medium with [1,2-^{13}C]-glucose for 24 hours. Extracted metabolites were analyzed by LC-MS/MS, and the percentage of ^{13}C-labeled nucleotides was compared. **(H)** Relative mRNA levels of pentose phosphate pathway genes from NHBE cells infected with AD WT or AD D68A for 12 hours at equal titer. For (B), (C), (E), (F), (G), and (H), error bars denote standard errors of the mean (n=3). * denotes $p<0.05$; ** denotes $p<0.01$ **(I)** Schematic representation of the shift in glucose metabolism upon infection with adenovirus. Upon infection with adenovirus, E4ORF1 binds to MYC and activates MYC-dependent transcription of metabolic genes to increase glycolytic flux and potential shunting of glucose metabolites into the non-oxidative arm of the PPP (to facilitate ribose biosynthesis for viral RNA production and DNA replication).